J Solid State Electrochem (2007) 11: 165–172
DOI 10.1007/s10008-005-0081-z

ORIGINAL PAPER

M. Jayalakshmi · P. Radhika
K. Phani Raja · M. Mohan Rao

Solvent and thiourea adsorption/intercalation effects on the solid-state electrochemistry of α-phase nickel hydroxide nanoparticles

Received: 6 September 2005 / Revised: 19 October 2005 / Accepted: 9 November 2005 / Published online: 17 December 2005

Abstract Nanoparticles of α-phase nickel hydroxide were synthesized by a single-step hydrothermal method using urea as the hydrolytic agent. Precipitated powders were of pure turbostratic α-phase as confirmed by x-ray diffraction profile. The ageing of α-$Ni(OH)_2$ in 1.0 M alkali solutions is investigated for pure non-intercalated α-$Ni(OH)_2$ and thiourea intercalated/absorbed α-phase nanomaterials. The α-$Ni(OH)_2$ powder immobilized on the surface of graphite electrodes shows a gradual α→β phase transformation with continuous voltammetric cycling, and the concentration gradient of water that exists in the layered-double-hydroxide-like interlayers of α-phase and the solution was shown to play a crucial role on the high electrochemical activity of this phase nickel hydroxide. To understand the role of water in the ageing process, concomitant entries of non-aqueous solvents like ethanol and acetonitrile along with thiourea were effected. Cyclic voltammetric measurements of thiourea-treated α-$Ni(OH)_2$ samples revealed that hydroxyl ion influx during the anodic oxidation depends on the counter flux of solvent molecules, and if the intercalated the solvent is acetonitrile, then the electrochemical activity of α-$Ni(OH)_2$ reduced drastically; $Q_a/Q_c>1$ for water as solvent in the interlayers α-$Ni(OH)_2$ and $Q_a/Q_c<1$ for ethanol and acetonitrile as solvents. The α-phase gets stabilized in the presence of thiourea with water and ethanol as co-intercalates. Transmission electron microscope images of α-$Ni(OH)_2$ and thiourea-treated samples show a change in particle size and morphology. Elemental CHNS analysis confirms the presence of sulphur in the thiourea intercalated samples.

M. Jayalakshmi · P. Radhika · K. P. Raja · M. M. Rao (✉)
Inorganic and Physical Chemistry Division,
Indian Institute of Chemical Technology,
Uppal Road,
Hyderabad 500 007, India
e-mail: mandapati@iictnet.org
Tel.: +91-40-27193510
Fax: +91-40-27160921

Keywords α-Nickel hydroxide nanoparticles · Water gradient · Thiourea and solvent intercalations · Solid state electrochemistry · Ageing

Introduction

The electrochemistry of nickel hydroxide has been well investigated, and exhaustive literature is available on this topic [1–5]. The prime application of nickel hydroxide as positive electrode material in rechargeable alkaline batteries has been the catalyst for the active interest of many researchers. To date, it is still one of the best electrode for rechargeable batteries. The major battery systems, Ni–Cd and Ni–MH are widely used in Walkman, compact disc, cassette players, camcorder, note book computers and electric vehicles. Nickel hydroxide has two polymorphs, namely, α- and β-$Ni(OH)_2$ which gets converted to γ-NiOOH and β-NiOOH, respectively, on oxidation, and the interlayer spacings for α-$Ni(OH)_2$, β-$Ni(OH)_2$,γ-NiOOH and β-NiOOH are 7.6 Å [6], 4.6 Å [7], 4.85 Å [8] and 7 Å [8, 9], respectively. With prolonged cycling, α-$Ni(OH)_2$ converts to β-NiOOH, which leads to mechanical strain, interlayer space volume and electrode capacity reduction which can happen either chemically or electrochemically or both, and the process is called ageing. Prevention of ageing is a primary concern and challenge for scientists, as α-phase gives higher capacity, and continual efforts are being made up to date in this direction. As a result, active research in understanding the ageing process has been pursued.

Open-circuit potential decay studies showed that the internal resistance of a stabilized α-nickel hydroxide electrode is lower than that of a β-nickel hydroxide electrode, while the charging efficient and the self-discharge followed the reverse trend [10]. An electrochemical quartz crystal microbalance (EQCM) study of mobile species transfer accompanying redox switching of electroprecipitated nickel hydroxide films exposed to aqueous lithium hydroxide solutions revealed that Li ions gets ejected during film oxidation and injected during reduction, while the solvent

molecules move in the opposite direction [11]. A combined EQCM and probe beam deflection (PBD) instrument was used to monitor mobile species transfers on short-time scales, following the application of a potential step to potentiostatically deposited α-nickel hydroxide films exposed to aqueous LiOH solution. It is found that upon film oxidation, hydroxide ions enter the film and protons are deintercalated. However, the protons are not detected directly since, upon ejection from the film, they immediately combine with hydroxide ions from the solution to yield water. As ions are driven into/out of the film to satisfy electroneutrality, the volume constraint causes solvent to be driven out of/into the film by internal pressure. The amount and dynamics of water expulsion at the interface are in part dependent on the free volume existing within the nickel hydroxide lattice. The rigid nature of the nickel hydroxide lattice imposes volume constraints, resulting in H_2O moving on the same time scale as ionic hydroxide and is no longer simply diffusionally controlled [12]. The mass responses for α- and β-phases were dramatically different, the reason being the difference in the dominant species; in the case of α-phase, hydroxide ion movement dominates, whereas in β-phase, H_2O movement dominates [13]. Infrared and x-ray diffraction (XRD) studies of α-Ni$(OH)_2$ showed that the usual formulation of α-Ni$(OH)_2$.nH_2O may not hold good; if the mother solution contains carbonate, nitrate, acetate ions, etc., the formula could be modified to accommodate these ions as α-Ni$(OH)_{2-x}A_yB_z$.H_2O, where A and B are mono or divalent anions and $x=y+2z$ [14]. In the case of zinc substituted α-Ni$(OH)_2$, most of the zinc was lost during ageing and on continuous cycling, the average interslab distance varies continuously from the value in the α-phase to that in the β-phase with the subsequent expulsion of water, carbonate, and nitrate and zinc ions [15]. Nuclear magnetic resonance (NMR) and Raman spectroscopic studies reveal that nitrate ions from the interlayer of α-Ni$(OH)_2$ are expelled within 5 min of ageing time in KOH solutions [16].

In our earlier communication, we reported the optimum conditions to synthesize α-Ni$(OH)_2$ nanoparticles by urea hydrolysis in high yields and phase pure form. Cyclic voltammetric studies in 1.0 M alkali solutions revealed that the electrochemical ageing occurs within 27 min (30 cycles) [17]. The α-Ni$(OH)_2$ is known to be turbostratic which means that the structure consists of brucite-type layer randomly oriented along the *c*-axis, which results from the lability of the water molecules located in the interlameller space [18]. Such lability in structure allows adsorption of even bigger anions like adipate, succinate which induces the expansion of interlayer distance as shown by XRD [14], and these observations confirm the fact that anions could be introduced into the interlayers of α-Ni$(OH)_2$ from the solution, a familiar procedure followed in layered double hydroxides (LDHs) or hydrotalcites. In such a situation, it would be interesting to study the effect of foreign entity (which do not induce any charge imbalance) with its solvation sheaths adsorbed/intercalated in the interlayers of α-Ni$(OH)_2$ on the redox transformations and reversibility, provided the solvents are of non-aqueous. The strategy is to incorporate a neutral molecule, for instance, thiourea from protic solvents (water, ethanol) and aprotic solvents, (acetonitrile) into the α-Ni$(OH)_2$ on the basis that the thiourea molecules would carry along the solvent molecules and study the redox behaviour in alkali solutions by cyclic voltammetry. This enables us to study the role of intercalated solvent as well as the thiourea molecules on the ageing process of α-Ni$(OH)_2$. Thiourea intercalated samples are characterized by XRD, transmission electron microscope (TEM) and CHNS analysis.

Experimental

Material preparation

Typically, $Ni(NO)_3.6H_2O$ (0.05 M) and urea (0.3 M) were dissolved in 200 ml of deionized water, and the solution was transferred to SS autoclave. It was programmed to reach 130°C in 1 h (ramp time), and at this temperature, the reaction was kept for 2 h (soak time) with stirring speed of 400 rpm. During the experiment, the in situ pressure developed was around 5–10 atm. When autoclave temperature reached to room temperature, the solution with precipitate was filtered and washed with distilled water to neutral pH. The solid was dried overnight in oven at 120°C to obtain α-phase Ni$(OH)_2$ nanoparticles.

Thiourea intercalated α-Ni$(OH)_2$ samples were prepared as per the standard protocol used in LDHs. To a 50-ml solution of thiourea (0.3 g), 1 g of α-Ni$(OH)_2$ nanoparticles was added and the solution was stirred continuously for 24 h. Then the product was filtered and washed well and dried in hot air oven. In a similar fashion, instead of water, ethanol and acetonitrile were used as solvents to prepared the thiourea intercalated α-Ni$(OH)_2$, and thus, obtained samples were designated as Ni-tu-w, Ni-tu-e and Ni-tu-a, respectively.

Instrumentation

All electrochemical experiments were conducted with a PGSTAT 30 Autolab system (Ecochemie, Utrecht, The Netherlands). It was connected to a PC running with Eco-Chemie GPES software. GPES software was used for all electrochemical data analysis. The reference electrode was an Ag/AgCl (3 M KCl) electrode, and the counter electrode was a platinum foil supplied along with the instrument. Paraffin-impregnated graphite electrodes (PIGE) were used as working electrodes with the surface immobilized with the active electrode materials. A few micrograms of α-Ni$(OH)_2$ nanoparticles were placed on a clean glass plate, and the surface of PIGE electrode was pressed over the nanomaterial which would mechanically transfer the nanoparticles to the tip of the electrode [19].

Powder XRD data of the samples were obtained by means of a Siemens D 5,000 XRD with Bragg–Brentano geometry and having Cu Kα radiation (λ=1.5418 Å). The samples were scanned for 2θ values in the range from 2° to

65°. TEM images were obtained with a PHILIPS make Tecnai-12 FEI instrument operated at an accelerating voltage of 100 kV. The $Ni(OH)_2$ samples were subjected to CHNS analysis. By this technique, the solids undergo combustion and the resulting gases were analysed.

Results and discussion

XRD studies

The XRD pattern of as-prepared α-$Ni(OH)_2$ nanoparticles was shown in Fig. 1. The XRD pattern shows the formation of phase pure α-phase of nickel hydroxide in concurrence with the earlier works [20]. The peak around 2θ=12, a landmark peak for the turbostratic nickel hydroxide and an asymmetric broad peak at about 2θ values of 32–35, characteristic of the turbostratic disorder, confirm the formation of pure α-phase. XRD patterns of the thiourea intercalated α-$Ni(OH)_2$ have clearly shown that all samples prepared in these conditions exhibit the turbostratic structure as revealed by the dissymmetrical line profiles of the *hk* bands (figures not given). There were no changes in the intersheet distance as evident from the position of 001 line. This could be due to planar arrangement of thiourea molecules similar to carbonate (source–urea from the preparative mixture) and nitrate ions whose presence does not alter the interlayer distance [14]. Though the presence of anionic species may raise the question of charge neutrality as in hydrotalcites, the presence of thiourea as uncharged molecule may not induce any charge excess. Nevertheless, the inductively coupled plasma (ICP) analysis of all samples revealed that the Ni content remains the same in spite of the presence of thiourea (results not given), and also the green colour of the intercalated precipitates excludes the possibility of Ni^{3+} defects in the interlayer.

Cyclic voltammetric studies of α-$Ni(OH)_2$ nanoparticles

Figure 2 shows the cyclic voltammograms of α-$Ni(OH)_2$ nanoparticles immobilized on the surface of a PIGE and exposed to 1.0 M NaOH solutions. Each electrode displays one anodic and one cathodic peak, corresponding to the $Ni(OH)_2 \leftrightarrow NiOOH$ redox reaction. The cyclic voltammetric (CV) shapes are not consistent even for pure α-$Ni(OH)_2$, and they change with increasing scans due to the expected ageing of α- to β-phase. The anodic peak appears larger and well defined than the cathodic peak at all scans. Table 1 presents the parameters derived from the CVs. The formal peak potential (E_f) is a measure of reversible potential and the difference in the anodic and cathodic peak potentials, and ΔE_p is a measure of the reversibility of the reaction. E_f values shift towards positive direction from the 1st to 50th scans, confirming the thermodynamic preference for the more stable β-phase. Ironically, ΔE_p also increases with cycling, an indication that the reversibility of the redox transformations decreased. It is a paradoxical situation but not unusual if one considers the complexity of the situation. The $Ni(OH)_2 \leftrightarrow NiOOH$ conversion itself is accompanied by influx of hydroxyl ions and outflux of water, protons, carbonate and nitrate ions in combination with ageing which proceeds by two separate but complimentary processes, namely chemical ageing in KOH solution and electrochemical ageing between oxidized and reduced states.

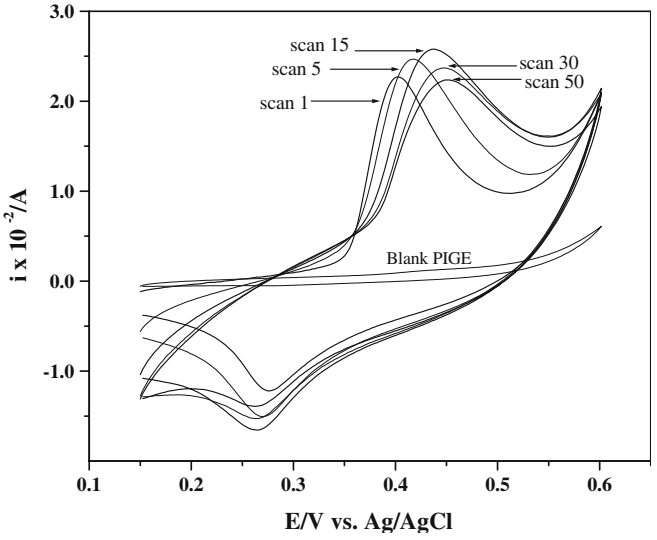

Fig. 2 Cyclic voltammograms of α-$Ni(OH)_2$ immobilized on paraffin-impregnated graphite electrode in 1.0 M NaOH solutions. Continuous cycling up to 50 scans

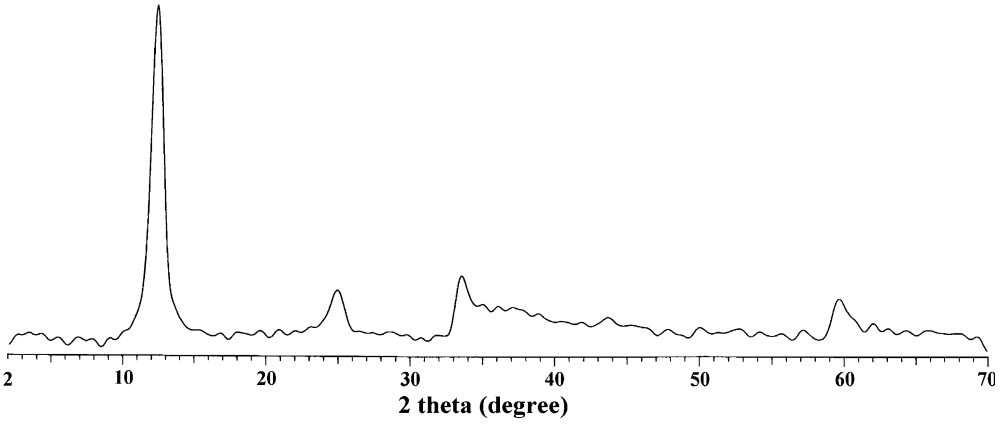

Fig. 1 XRD pattern of phase pure α-$Ni(OH)_2$ nanoparticles synthesized by hydrothermal method

Table 1 Parameters obtained from the cyclic voltammetrics (CV) of pure α-$Ni(OH)_2$ in 1.0 M NaOH solutions

Cycle number	E_a (mV)	E_c (mV)	ΔE_p (mV)	E_f (mV)	Q_a ($\times 10^{-3}$ C)	Q_c ($\times 10^{-3}$ C)	Q_a/Q_c	DOP (mV)
1	401	277	124	336	6.801	4.481	1.52	199
5	414	270	144	342	8.150	4.754	1.71	186
15	433	267	166	350	8.105	4.028	2.01	167
30	441	267	174	354	6.694	2.535	2.64	159
50	445	270	175	357	6.382	1.821	3.50	155

The difference between the oxygen evolution potential and the oxidation peak potential (DOP) is used as a measure of oxygen evolution over potential. The highest value of DOP is observed for the initial scan but decreased considerably for the 50th scan. Oxygen evolution over potential is an unwanted parasitic reaction during the charging of alkaline batteries, and higher DOP is more desirable for the performance of $Ni(OH)_2$ electrode. In this aspect, α-phase has distinct advantage as against the β-phase. It could be seen that the E_a (anodic peak potential) shifts towards positive direction, while the E_c (cathodic peak potential) remains almost constant. The anodic peak occurs due to the following oxidation reaction:

$$Ni(OH)_2 + OH^- \rightarrow NiOOH + H_2O + e^- \quad (1)$$

Hydroxyl ions are intercalated during this step, and the protons were deintercalated with the outflux of water molecules. This could be confirmed by the fact the Q_a/Q_c charge ratio being greater than 1; this happens due to the excess capacity of OH^- ions inserted into the nickel hydroxide layers (Table 1). As $Q_a > Q_c$ at all scans, the anodic oxidation occurs more readily than the cathodic reduction.

This redox reaction can be rewritten as,

$$H_nNiOOH \leftrightarrow NiOOH + nH^+ + ne^- \quad (2)$$

A significant and interesting fact was the increase in anodic charge from the first (6.8×10^{-3} C) to 15th scan (8.15×10^{-3} C) and decreased at the 30th scan (6.69×10^{-3} C). This increase in charges under the anodic peak may be attributed to the electrochemical activity of water molecules associated with protons, and the process can be described as follows.

On anodic polarization, OH^- ions move towards the film/solution interface as

$$(OH^-)_B \leftrightarrow (OH^-)_S \quad (3)$$

where B is the bulk of the solution and S is the surface of the film. Depending on the local electrical field and thickness of diffusion of OH^- ions from the surface to some site in the interior of the film, the following reaction occurs:

$$(OH^-)_S \leftrightarrow (OH^-)_I \quad (4)$$

The oxidation of divalent hydroxide releases the proton which diffuses away from the electrode to a site in the oxide where it combines with the OH^- ion to form water.

$$(H^+)_I \rightarrow (H^+)_n \quad (5)$$

$$(H^+)_n + (OH)^-_n \rightarrow (H_2O)_n \quad (6)$$

where n is the neutralization site. As oxidation proceeds, the neutralization site moves towards the solution site, and the progress of the neutralization site ceases as it reaches the solution phase. This explains the presence of water concentration gradient in the film, and the variation in the electrochemical activity could be associated with water activity in the solid phase [17]. After 30th scan, the concentration gradient between the solid phase and solution ceases, and equilibrium was established with a decrease in water concentration in the solid phase (beta-phase), thus explaining the almost constancy of peak charges and potential up to 50th scan.

In addition to the role of water molecules deciding the thermodynamic stability, the concomitant phase transformations of α-$Ni(OH)_2$ may decide the high anodic charges. Figure 3 illustrates the reaction scheme of nano-α-$Ni(OH)_2$

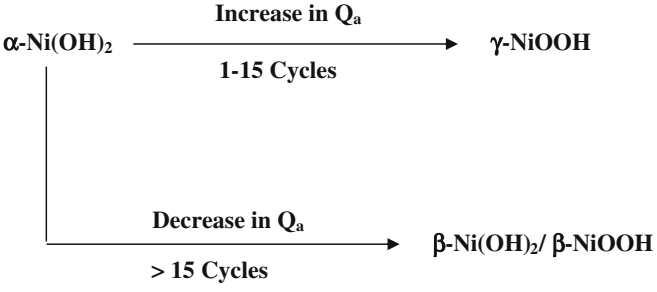

Fig. 3 Scheme for the conversion of alpha to beta nickel hydroxide on electrochemical cycling

Table 2 Parameters obtained from the CVs of Ni-tu-w sample in 1.0 M NaOH solutions

Cycle number	E_a (mV)	E_c (mV)	ΔE_p (mV)	E_f (mV)	Q_a ($\times 10^{-3}$ C)	Q_c ($\times 10^{-3}$ C)	Q_a/Q_c	DOP (mV)
1	375	272	103	324	3.493	3.309	1.06	145
5	384	267	117	325	4.991	4.359	1.15	136
15	411	255	156	333	8.732	7.030	1.24	109
30	421	248	173	335	8.350	7.420	1.13	99
50	426	243	183	335	8.464	6.607	1.13	94

in 1 M NaOH during the 50 scans of continuous cycling. This scheme explains the rationale behind the increase in Q_a values in the initial 1–15 cycles, stabilizing up to 30 cycles and then started decreasing thereupon. Nano-α-Ni $(OH)_2$ is converted into γ-NiOOH, which leads to an increase in anodic charges, as the γ-phase also is an open structure like α-phase with a *c*-axis spacing of about 20 Å that can accommodate easily water molecules or alkali metal cations. With increase in cycling, conversion of α- to β-NiOOH causes decrease in interslab distance which curtails the ion fluxes, and the anodic peak charges starts declining [21]. The conversion of β-NiOOH into γ-NiOOH cannot be taken into consideration in the present study, as it happens only in very high concentrations of alkali.

The consistent increase in Q_a/Q_c charge ratio with continuous cycling could be explained based on the nickel vacancies within NiO_2 slabs in non-substituted α-phase and to ensure charge compensation on prolonged cycling to convert α- to β-phase, either some additional protons are intercalated or some nickel ions are oxidized in which case, $Q_a/Q_c>1$ is expected. Like the starting α-phase, the resulting β-phase must contain octahedral vacancies as the transformation occurs only in the solid state [22].

CV studies of α-$Ni(OH)_2$ nanoparticles intercalated with solvent and thiourea

Ni-tu-w

The CVs recorded for this sample under identical conditions as that of pure α-$Ni(OH)_2$ would reflect the changes incurred due to the intercalation of thiourea along with solvent water molecules. As the solvent in this case is water, the effect of it on the ageing process may not differ significantly from that described for that of pure α-phase. Table 2 shows the parameters derived from the CVs recorded in the 1st to 50th scans, and the respective CVs were shown in Figs. 4 and 5. Intercalation of thiourea in the slabs of α-phase was responsible for the noticeable negative shift of the anodic peak in the 1st scan, and the trend continues in all the subsequent scans. The cathodic peak also shifts towards negative direction, and the shift is significant at all scans as against pure phase so that the ΔE_p values are comparatively higher, a pointer to decreasing reversibility. E_f also shifted towards negative direction, though the increment was much smaller compared to charge value. DOP decreased with increasing scans, and as such, DOP

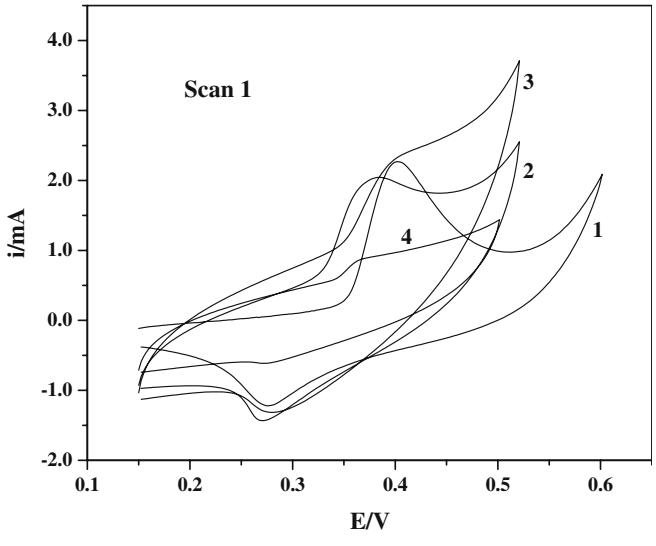

Fig. 4 Cyclic voltammograms of α-$Ni(OH)_2$ (*curve 1*), Ni-tu-w (*curve 2*), Ni-tu-e (*curve 3*), Ni-tu-A (*curve 4*) for the first scan in 1.0 M NaOH solutions

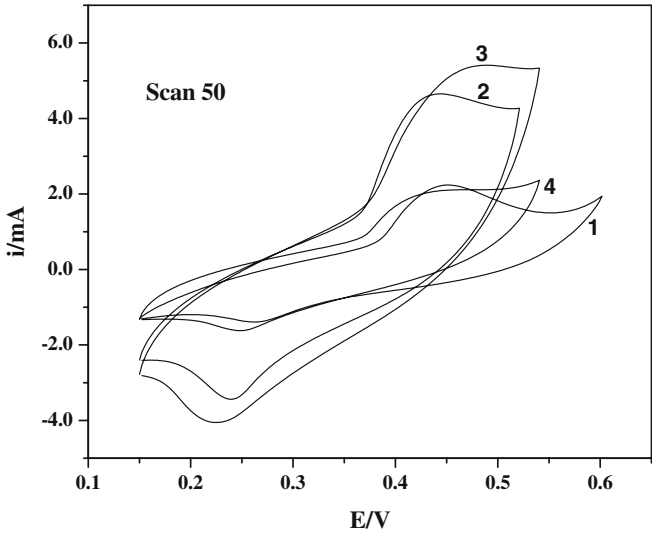

Fig. 5 Cyclic voltammograms of α-$Ni(OH)_2$ (*curve 1*), Ni-tu-w (*curve 2*), Ni-tu-e (*curve 3*), Ni-tu-A (*curve 4*) for the 50th scan in 1.0 M NaOH solutions

Table 3 Parameters obtained from the CVs of Ni-tu-e sample in 1.0 M NaOH solutions

Cycle number	E_a (mV)	E_c (mV)	ΔE_p (mV)	E_f (mV)	Q_a ($\times 10^{-3}$ C)	Q_c ($\times 10^{-3}$ C)	Q_a/Q_c	DOP (mV)
1	397	287	110	342	1.858	2.477	0.75	123
5	399	279	120	339	2.856	3.799	0.75	121
15	421	257	164	339	5.398	7.268	0.74	99
30	436	248	188	342	7.517	8.663	0.87	84
50	450	233	217	342	8.209	9.073	0.91	70

is favourable in the pure phase rather than in Ni-tu-w. Interestingly, Q_a value was much lower in the first scan, increased in the subsequent scan and reached a maximum value in the 15th scan and thereupon remained almost constant. In contrary to the pure α-$Ni(OH)_2$ phase as shown in Table 1, the values did not decrease after the 15th scan, an indication that the ageing process is not favoured. Finally, Q_a/Q_c values are equal to 1 in the first scan and become greater than 1 in the subsequent scans, indicating that the anodic reaction occurs more favourably with cycling. However, the magnitude of readiness with which the anodic reaction occurs decreased in Ni-tu-w.

As the solvent being water in both the solid and solution phase, the changes observed could be only due to the presence of thiourea in the slabs of α-$Ni(OH)_2$. Comparing the Q_a values at the 30th and 50th scans for pure α-$Ni(OH)_2$ and Ni-tu-w samples, it is clear that the anodic charges did not decrease in the Ni-tu-w, a fact which symbolizes the stabilization of α-phase. Assuming the ageing process occurs as predicted in the scheme (Fig. 3), it is more probable that the presence of thiourea helps to prevent the leaching of water molecules from the interlayer by enhanced hydrogen bonding so that the conversion of α- to β-phase did not occur readily in Ni-tu-w sample.

Ni-tu-e

In this sample, α-$Ni(OH)_2$ has two foreign species, i.e. thiourea and ethanol. As the thiourea enters the slabs of nickel hydroxide, it is well known that concomitant entry of solvent molecules cannot be avoided. In such a situation, along with thiourea, ethanol also plays a role in the redox characteristics of α-$Ni(OH)_2$ in alkali solutions. This is proved to be true. Table 3 shows the parameters obtained from the CVs for Ni-tu-e in 1.0 M NaOH solution for the continuous 50 scans. The anodic peak potential did not shift significantly, as against the pure phase and in the subsequent scans, the trend remained the same. This is a pointer to dominance of ethanol in deciding the redox characteristics of $Ni(OH)_2 \leftrightarrow NiOOH$ rather than thiourea molecules. The DOP changed dramatically and adverse to the NOE electrode, as minimum DOP signifies a reduction in over potential for oxygen evolution, which in turn would affect the charging efficiency of the NOE. On the other hand, it could be predicted as a beneficial observation as oxygen evolution is a perquisite for fuel cell electrode.

The most interesting result is the Q_a/Q_c values; the ratio is less than 1 up to the 50th cycle, which indicates the cathodic dominance involving the influx of protons. This observation is contrary to the pure α-$Ni(OH)_2$ and Ni-tu-w samples where the influx of hydroxyl ion during the anodic oxidation was the predominant process. The reason for this anomaly could due to the presence of ethanol in the interlayers of α-$Ni(OH)_2$ which seem to hinder the agile traffic of hydroxyl ions towards the interface. Presence of ethanol in the interlayers, though hydrophilic, the nature and energetics of hydrogen bonding between the hydroxyl ions of ethanol and that of alkali and water molecules may not encourage the simultaneous hydrogen bond breaking and formation, a absolute necessity for free movement of either protons or hydroxyl ions. This explains the decrease in peak currents for this sample. During reduction, for charge compensation, protons/sodium ions are required, as the presence of ethanol occupying space volume in the interlayers reduces the interlayer water content, increasing the proton/Na^+ ion traffic across the interface, leading to $Q_a/Q_c < 1$.

Ni-tu-a

In this sample, instead of ethanol, we have acetonitrile and thiourea in the interlayer of α-$Ni(OH)_2$. Acetonitrile is an aprotic solvent, and the formation of hydrogen bonding between the interlayer water molecules, protons, hydroxyl ions and acetonitrile cannot be expected. Table 4 shows the parameters derived. Q_a value for the first scan is abnor-

Table 4 Parameters obtained from the CVs of Ni-tu-a sample in 1.0 M NaOH solutions

Cycle number	E_a (mV)	E_c (mV)	ΔE_p (mV)	E_f (mV)	Q_a ($\times 10^{-3}$ C)	Q_c ($\times 10^{-3}$ C)	Q_a/Q_c	DOP (mV)
1	365	279	86	322	0.351	0.466	0.75	170
5	372	279	93	326	0.537	0.689	0.77	163
15	387	275	112	331	1.022	1.158	0.88	148
30	409	262	147	336	2.572	2.720	0.95	126
50	421	253	168	337	2.766	2.891	0.96	114

Table 5 CHNS elemental analysis of α-$Ni(OH)_2$ and thiourea intercalated samples

Sample	CHNS analysis (%)		
	Carbon	Nitrogen	Sulphur
α-$Ni(OH)_2$	5.86	3.91	–
Ni-tu-w	5.21	4.39	0.58
Ni-tu-e	5.48	4.75	1.06
Ni-tu-a	5.59	4.34	1.44

mally less and with continuous cycling, it increases but never reached the higher value as in the other samples. The value is much lesser than that of Ni-tu-e sample, and the reason behind this behaviour of NOE electrode could be ascertained to aprotic nature of the solvent concomitantly exist in the slabs. The hydrophobic environment created by the acetonitrile in the interlayers of α-$Ni(OH)_2$ hinders to a large extent the facile flux of protons, hydroxyl ions and water molecules.

Ni-tu-a sample behaves in a unique fashion with respect to the thiourea intercalation. While in the Ni-tu-e sample, the presence of thiourea by the obvious shift in anodic peak potential is not observed, it happens in the Ni-tu-a sample (E_a=365 mV). Also, ΔE_p is less compared to all the three samples indicating an increase in reversibility of NOE reaction. DOP is reasonably higher than the Ni-tu-e and Ni-tu-w samples.

Effect of cycling

The effect of cycling could be understood from the cyclic voltammograms shown in Figs. 2, 4 and 5. It is quite interesting to analyse the effect of continuous cycling in all the non-intercalated and thiourea intercalated samples. DOP, irrespective of the presence of thiourea, decreased from the 1st to 50th scans for all the samples. On the other hand, Q_a increased in the same order, though the magnitude depended on the solvent. Also, Q_a/Q_c charge ratio increased with cycling whether it is less than or greater than 1. This explains that α-$Ni(OH)_2$ undergoes complex physical and structural changes during potential cycling. Increase of Q_a/Q_c charge ratio implies a growth of active nickel hydroxide at the electrode surface. For all the samples, ΔE_p increased with cycling, a pointer to reduction in reversibility. E_a shifted towards positive direction for all the samples with increase in scans. This is expected for the ageing of α-$Ni(OH)_2$ in alkali solutions and is consistent with that reported in an earlier work; the anodic peak for α-phase appeared at 449 mV vs Hg/HgO, while the aged β-phase appeared at 514 mV [23].

Effect of solvents on ageing

Stabilization of Q_a values (Tables 1, 2, 3 and 4) could be taken as a landmark for retarding or slowing down the ageing process; this happened in all the thiourea intercalated samples at and after the 30th cycle. In the case of ethanol and acetonitrile as co-intercalated solvents, the obvious difference in Q_a values (rather a considerable decrease for acetonitrile) signifies the hydrophobic environment provided by acetonitrile inhibiting the hydroxyl ion transfer from the solution to the electrode. Ironically, it has prevented ageing in a destructive fashion, but ethanol has done the same with a constructive manner as it does not break down the hydrogen bonding network essential for hydroxyl ion traffic.

CHNS analysis

Table 5 shows the results of CHNS analysis of pure α-$Ni(OH)_2$ and thiourea-treated samples. As expected, there was no sulphur in the pure sample; the presence of nitrogen and carbon has their origin from the preparative mother solutions. Interestingly, the amount of sulphur was the highest in Ni-tu-a sample. Comparing water and ethanol co-intercalated samples, the sulphur content was higher in the case of Ni-tu-e than in Ni-tu-w.

TEM studies

Figure 6a shows the TEM image of as-prepared α-$Ni(OH)_2$ nanoparticles, and they are of non-uniform in size and shape, which is expected as the nanomaterial was prepared in the absence of structure directing agents. The tendency of nanoparticles to agglomerate is indicated by the dark patches in the TEM images. The α-$Ni(OH)_2$ particle

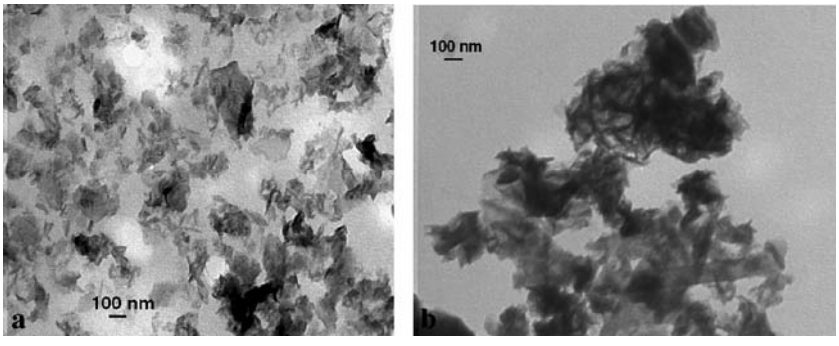

Fig. 6 TEM image of (**a**) as-prepared α-$Ni(OH)_2$ nanoparticles by hydrothermal method; (**b**) Ni-tu-e sample; α-$Ni(OH)_2$ nanoparticles after exposed to thiourea dissolved in ethanol for 24 h

sizes varied from 50 to 200 nm. Figure 6b shows the TEM images of Ni-tu-e sample. There is a vast difference in the morphology, and interestingly, the nanoparticles had self-assembled to rod-like shapes and the tendency to aggregate has been increased. This difference in shape and size of Ni-tu-e sample could be ascertained to the addition to thiourea and ethanol which have acted as structure directing agents. Such self-assembly of hydrotalcite nanoparticles in the presence of carbonate ions, leading to overlapping layers with time, thus forming a three-dimensional network, has been reported very recently [24].

Conclusions

This study on the electrochemical ageing of α-$Ni(OH)_2$ to β-$Ni(OH)_2$ in 1.0 M NaOH solutions revealed interesting observations; the concentration gradient of water that exists between the solid and the solution enhances the electrochemical activity of α-$Ni(OH)_2$, and as the gradient ceases to exist with cycling, the α-phase changes to β-phase. The ageing process gets affected by the presence of thiourea in the interlayers. CHNS analysis of thiourea-treated samples, and their CV responses confirm the intercalation of thiourea with its solvation sheath into the interlayers of α-$Ni(OH)_2$. Firstly, thiourea stabilized the alpha-phase in the case of Ni-tu-w and Ni-tu-e samples, and the peak currents did not decrease up to the cycled 50 scans. Though, the mechanism changed as the solvent changed from water to ethanol, the stability of alpha-phase remained. In Ni-tu-w sample, hydroxyl influx during anodic oxidation dominates the charge transfer reaction, while in Ni-tu-e sample, proton influx during cathodic reduction dominated the reaction. Drastic reduction in electrochemical activity was noticed for Ni-tu-a sample; this is expected due to the aprotic nature of acetonitrile breaking down the network of hydrogen bonding, thus hindering the traffic of hydroxyl ions and protons to and from the interlayers to the interface.

References

1. Hana XJ, Xua P, Xua CQ, Zhaoa L, Moa ZB, Liu T (2005) Electrochim Acta 50:2763
2. Meyer M, Bée A, Talbot D, Cabuil V, Boyer JM, Répetti B, Garrigos R (2004) J Colloid Interface Sci 277:309
3. Liu X, Yu L (2004) Mater Lett 58:1327
4. Carter JC, Khulbe PK, Gray J, Van Zee JW, Angel SM (2004) Anal Chim Acta 514:241
5. Srinivasan V, Weidner JW, White RE (2000) J Solid State Electrochem 4:367
6. Le Bihan S, Guenot J, Figlarz M (1970) C R Acad Sci Ser C 270:2131
7. McEwen RS (1971) J Phys Chem 75:1782
8. Oliva P, Leonardi J, Laurent JF, Delmas C, Braconnier JJ, Figlarz M, Fiev F, Deguibert A (1982) J Power Sources 8:229
9. O'Grady WE, Pandya KI, Swider KE, Corrigan DA (1996) J Electrochem Soc 143:1613
10. Ganesh Kumar V, Munichandraiah N, Vishnu Kamath P, Shukla AK (1995) J Power Sources 56:111
11. Gonsalves M, Robert Hillman A (1998) J Electroanal Chem 454:183
12. French HM, Henderson MJ, Hillman AR, Vieil E (2002) Solid State Ionics 150:27
13. French HM, Henderson MJ, Hillman AR, Vieil E (2001) J Electroanal Chem 500:192
14. Delahaye-Vidal D, Beaudoin B, Sac-Epee N, Tekaia-Elhsissen K, Audemer A, Figlarz M (1996) Solid State Ionics 84:239
15. Tessier C, Guerlou-Demourgues L, Faure C, Basterreix M, Nabias G, Delmas C (2000) Solid State Ionics 133:11
16. Bernard MC, Bernard P, Keddam M, Senyarich S, Takenouti H (1996) Electrochim Acta 41:91
17. Jayalakshmi M, Venugopal N, Ramachandra Reddy B, Mohan Rao M (2005) J Power Sources 150:272
18. Genin P, Delahaye-Vidal A, Portemer F, Tekaia-Elhsissen K, Figlarz M (1991) Eur J Solid State Inorg Chem 28:505
19. Scholz F, Meyer B (1998) Voltammetry of solid microparticles immobilized on electrode surfaces. In: Bard AJ, Rubinstein I (eds) Electroanalytical chemistry, a series of advances, vol 20. Dekker, New York, p 1
20. Bing L, Huatang Y, Yunshi Z, Zuoxiang Z, Deying S (1999) J Power Sources 79:277
21. Kostecki R, McLarnon F (1997) J Electrochem Soc 144:485
22. Jeong DJ, Kim WS, Choi YK, Sung YE (2001) J Electroanal Chem 511:79
23. Kim MS, Hwang KB, Kim J (1997) J Electrochem Soc 144:1537
24. Choudary BM, Swarna Jaya V, Ramachandra Reddy B, Lakshmi Kantam M, Mohan Rao M, Sakunthala Madhavendra S (2005) Chem Mater 17:2740